April 27, 2022

Sunspot numbers and proton events in solar cycles 19 to 24.

M. J. Birch, B. J. I. Bromage

Jeremiah Horrocks Institute for Mathematics, Physics and Astronomy,

University of Central Lancashire, Preston, UK.

Abstract

In this study we compare the mean annual sunspot numbers for the six most recent solar cycles (19 to 24) with the number of solar energetic proton events occurring in those years. Though most of the individual cycles exhibit quite strong correlations, when they are combined into a generic solar cycle the result is very significant ($\rho = 0.98$). For cycles 21 to 24 (when spacecraft observations have been regularly available), we also investigate the variation in the source location of the solar energetic proton events in relation to four peak flux thresholds in orders of magnitude from $\geq$10 to $\geq$10000 pfu, For helio-latitudes within $\pm 40^\circ$ (the range within which active regions usually occur) there is negligible variation in the helio-longitude of the source regardless of the peak flux threshold. However, the effect on the helio-longitude of varying the peak flux threshold is very significant: the higher the threshold

the closer is the median source longitude to 0°, the variation being almost uniform from ≥10 pfu (32°W) to ≥10000 pfu (2°W). Finally, of the 10 events in cycles 19 to 24 with peak flux ≥10000 pfu, all occurred between years 4 and 8 after solar minimum, all were the result of M- or X-class flares with associated halo CMEs and shock fronts, and the three most intense events (≥40000 pfu) were all related to X-class flares which occurred in the longitude range 10-28°E. These results support and extend previous work by the cited authors, and have implications for solar-terrestrial relations and the effects of space weather within geospace.

1 Introduction

Sunspots are temporary phenomena on the photosphere of the Sun that are caused by intense magnetic activity which inhibits convection, forming areas of reduced surface temperature. They usually appear as pairs, with one sunspot having the opposite magnetic pole to the other. Although they have temperatures of ≈3000-4500 K, the contrast with the surrounding material at ≈5780 K leaves them clearly visible as dark spots, the luminous intensity of a heated black body (closely approximated by the photosphere) being a function of temperature to the fourth power. Sunspots expand and contract as they move across the surface of the Sun and can be as small in diameter as 16 km and as large as 160,000 km. They may also travel at proper motions of a few hundred metres per second when they first emerge on to the solar photosphere. Manifesting intense magnetic activity, sunspots host secondary phenomena such as coronal loops, prominences and reconnection events, initiated by re-structuring of the local magnetic field (van Speybroeck et al., 1970). Solar flares and coronal mass ejections (CMEs), the result of such reconnection events, originate in magnetically active regions around sunspot groups, and are the primary source of solar energetic protons (Gabriel et al., 1990).

The sunspot number (Section 2.1), the index most commonly used to estimate solar activity, has a mean periodicity of about 11 years, with a maximum variation of between 8 and 15 years

since observations first began in 1749. This solar activity cycle has an asymmetric form, the average rise to maximum taking 4.8 years compared with 6.2 years for the fall to minimum. The latitudinal variation of sunspots correlates with the sunspot number: sunspots usually occur between latitudes 40°N and 40°S and migrate from high to low latitudes as the solar cycle progresses, resulting in the butterfly diagram (Ivanov, 2018). Indeed, in our data, the source of only 1 SEP event in 233 has been identified beyond these latitude limits.

In this study we focus on the 6 most recent solar cycles (19 to 24), during which we compare the mean annual sunspot number with the number of solar energetic proton (SEP) events occurring in each of those years. For cycles 21 to 24, we also consider how the source location of SEP events on the solar disc varies with respect to their peak flux threshold, in orders of magnitude from ≥10 to ≥10000 pfu (particle flux units, $cm^{-2}.s^{-1}.sr^{-1}$). The implications for space weather are also considered, particularly with regard to the 10 events with peak flux ≥10000 pfu which have occurred during the 6 cycles.

(Throughout this paper, all references to pfu assume >10 MeV protons.)

2 Data provision

The internet sites for the two data providers below are listed in the Acknowledgements.

2.1 Sunspot numbers

The sunspot number (SSN) is a commonly used index of solar activity. The daily SSN was first introduced in 1848 by the Swiss astronomer Johann Rudolph Wolf. His method, which is still used today, counts the total number of spots visible on the face of the Sun and the number of groups into which they cluster, because neither quantity alone is satisfactory for measuring sunspot activity.

The relative SSN is an index of the activity of the entire visible disk of the Sun. It is determined each day without reference to preceding days, and is defined as $R = K(10g + s)$, where g is the number of sunspot groups and s is the total number of distinct spots. The scale factor K (usually less than unity) depends on the observer and is intended to normalise the conversion to the scale originated by Wolf (Cliver et al., 2013).

The provisional daily Zurich relative SSNs (R_z) were originally based upon observations made at Zurich and its two branch stations in Arosa and Locarno, Switzerland. Beginning January 1 1981, this system was replaced by the provisional international SSN (R_i) based on a statistical treatment of the data originating from more than twenty-five observing stations. These stations constitute an international network, with Locarno as the reference station, to guarantee continuity with the earlier Zurich system. The definitive international SSNs are evaluated by a similar method based on a network of observing stations selected for their high number of observations, their continuity during the whole year, and an existing series of observations for past years. Also taken into account is the stability of the monthly factor (K) with reference to the Locarno station. Each SSN monthly average is simply the mean of the daily values.

Over the years many sunspot number data sets have been provided by various observatories. The current accepted standard is the Sunspot Index and Long-term Solar Observations (SILSO) catalogue from the Royal Observatory of Belgium, Brussels, and in our study we have used the monthly mean total sunspot number from this catalogue. On July 1st, 2015, a new improved version was published that includes several corrections of past inhomogeneities in the time series (Clette et al., 2014; Clette and Lefèvre, 2016a; Clette et al., 2016b; Clette et al., 2016c). Most significant is the removal of the Zurich scale factor (0.6), thus increasing the entire time series by a factor 1/0.6, to the level of modern sunspot counts. This scale change, when combined with the recalibration, leads to an average increase of about 45% of the most recent part of the

series, after 1947 (the period applicable to this study).

The start and end of each solar activity cycle are defined by the minima in the monthly average sunspot numbers. The start and end dates of solar cycles 19 to 24, and the duration in months and years (whole and part) of each cycle, are given in Table 1. The cycles vary in duration from 121 months (cycle 22) to 146 months (cycle 23).

Cycle	Start	End	Months	Years	SEP source	No. of SEPs	ρ
19	May 54	Oct 64	126	11	[1]	65	0.79
20	Nov 64	Jun 76	140	12	[1]	72	0.79
21	Jul 76	Sep 86	123	11	[2], [1]	58, 81	0.55, 0.58
22	Oct 86	Oct 96	121	11	[2]	73	0.94
23	Nov 96	Dec 08	146	13	[2], [3]	92, 103	0.86, 0.80
24	Jan 08	Dec 19	132	11	[2]	36	0.73
Total						396, 430	

Table 1: Solar cycles 19 to 24: start and end date, duration in months and years (whole or part), sources of event SEP data ([1] Shea and Smart, 1990. [2] Space Weather Prediction Centre. [3] Cane et al., 2006), number of SEP events, and correlation coefficient between the mean annual SSN and the annual number of SEP events.

2.2 Solar energetic proton events

"Solar cosmic rays" were first detected by Forbush in 1942 using Compton Bennett meters (Forbush, 1946), which are ionization chambers (the energies associated with these particles being in the GeV range). By the late 1950s ground-based measurements in the >10 MeV range became possible using riometers (Little and Leinbach, 1959), and most of the solar particle flux

and fluence data available from the 19th solar cycle were derived from such measurements, in the polar regions. Although spacecraft measurements of SEP events were made towards the end of solar cycle 19, it was not until cycle 20 that these measurements became routine.

For our investigation of the SEP events in cycles 19 to 24 we have used three sources: [1] Shea and Smart, 1990 (January 1955 to May 1986, covering cycles 19 to 21); [2] the Space Weather Prediction Centre (SWPC) SEP catalogue (April 1976 to date, covering cycles 21 to 24); [3] Cane et al., 2006 (November 1997 to September 2005, covering most of cycle 23). (We were unable to identify any peer-reviewed SEP event lists for cycles 22 or 24.)

Shea & Smart (1990) admit that it was not possible to compile a completely homogeneous list of solar proton events for cycles 19 and 20, primarily because of the different measurement techniques used prior to 1976 (both ground- and space-based). Nevertheless, they state that their list is as homogeneous as possible. In their list, Shea & Smart do not include solar source locations, and only list >10 MeV fluxes from May 1967, an event from this date only being included if particles of this energy measured a flux of ≥10 pfu.

Since the start of cycle 21 in 1976 the NOAA SWPC has maintained a standardised catalogue of SEP events. The proton fluxes are integral 5-minute averages for energies >10 MeV measured by the GOES series of spacecraft at geosynchronous orbit. The parameters for each event include:

1. the start and peak UTC of each particle event, and the peak flux;
2. details of any associated CMEs (available from SOHO since 1996);
3. details of the source flare and associated active region (UT of flare maximum, flare classification, source location (helio-latitude and -longitude), and active region number).

(For reasons of brevity, *latitude* and *longitude* will subsequently be used instead of *helio-latitude* and *helio-longitude*.) The head of the SWPC has advised that the curator of the SEP event

catalogue regularly collaborates with staff at the NASA Space Radiation Analysis Group to ensure the fidelity of the event data (private communication).

The SWPC defines the start of a SEP event to be marked by the first of 3 consecutive data points at >10 MeV with fluxes ≥10 pfu, and the end of the event to be the last data point with flux ≥10 pfu. This definition allows multiple proton flares and/or interplanetary shocks to be included within a single event, and differs somewhat from the Shea and Smart criterion for commencement of each event (this will have implications below). (The SWPC issue a point of caution: "Different detectors aboard different GOES spacecraft have taken the data since 1976. These proton data were processed using various algorithms. To date no attempt has been made to cross-normalize the resulting proton fluxes".)

Because of the different approaches used to identify individual SEP events in the three sources, particularly the starting criteria, there are inevitable inconsistencies between the number of events in some years of cycles 21 and 23. For example, in cycle 21 Shea and Smart identify 81 events, whereas there are only 58 in the SWPC catalogue. Inspection of the two sources reveals that this discrepancy results from the fact that the SWPC marks the start of an event by 3 consecutive data points >10 MeV with fluxes ≥10 pfu, whereas Shea and Smart do not impose this 3-point restriction. Consequently, Shea and Smart include 15 events not listed by SWPC and 11 that are components of those in the SWPC list. Conversely, 3 events included by SWPC are not listed by Shea and Smart.

There are also discrepancies between the SEP events from November 1997 to September 2005 listed by Cane et al. (2006) and those in the SWPC catalogue for the same period (numbering 101 and 90, respectively). (This period excludes the 2 events from December 2006 at the end of cycle 23.) Four of the events listed by Cane et al. are not in the SWPC catalogue, 7 are components of those in the SWPC events, and 3 are included by the SWPC but not by Cane

et al. In addition, 5 events listed by Cane et al. replace two in the SWPC catalogue in 2005 (January 16 and July 14). Of particular note are the 3 events which replace the one on July 14 listed by the SWPC (the ambiguous nature of this activity is detailed specifically in a footnote). Of those events common to both lists, only 11 (less than 5%) differ in source location, and only 2 (less than 1%) differ in peak flux intensity, and it will be shown that the effect of these differences on the overall results is not significant.

For SEP events in solar cycles 19 and 20 (137 events), in this study we have used the list provided by Shea & Smart (1990), and for cycles 21 to 24 we have used the SWPC catalogue because it is the only single source covering this whole period (this choice will subsequently be referred to as *selection 1*). (There are precedents in the peer-reviewed literature for using this catalogue, such as Cheng et al., 2014, Le et al., 2014 and Le et al., 2021.) However, because of the inconsistencies detailed above, throughout the analysis we have tested the effect of using Shea and Smart (1990) for cycle 21 and Cane et al (2006) for cycle 23 (this choice will subsequently be referred to as *selection 2*). It will be shown that the results from selections 1 and 2 are very similar, thus demonstrating that the outcome is robust.

Throughout the paper, various groups of SEP events are selected from the three sources using different criteria. For clarification, a table summarising these selections and sample numbers is provided in the Appendix.

3 Comparison of annual sunspot numbers and proton events in cycles 19 to 24.

The total number of SEP events recorded during solar cycles 19 to 24 (Table 1) are 396 (selection 1) and 430 (selection 2). Figure 1 shows a comparison between the number of SEP events per year (from selection 1) and the mean annual SSN for each of the 6 solar cycles,

measured in years from sunspot minimum. (The red dotted lines, discussed in Section 5.1, indicate ≥10000 pfu events.) Though the overall intensity of solar activity changes from cycle to cycle, in most cases the variations in the two quantities are not dissimilar. The linear Pearson correlation coefficients are given in Table 1 (column 8), cycle 22 having the highest coefficient (0.94) and cycle 21 the lowest (0.55 for selection 2). Evidently the two quantities are in general quite well correlated, though the efficacy of predicting one quantity from another will clearly vary from cycle to cycle (Shea and Smart, 1990). It is also shown in Table 1 that, for each of cycles 21 and 23, the correlations for the two alternative selections are quite similar.

The effect of superposing the selection 1 data from the 6 cycles is shown in Figure 2. There are 69 samples, one for each year (whole or part) of each solar cycle (Table 1), and they give quite a strong linear Pearson correlation ($\rho = 0.74$). The annual number of SEP events (p) is related to the mean annual sunspot number (s) according to the central regression line equation for a least-squares fit:

$$p = 0.080s - 1.416 \tag{1}$$

These data are heteroskedastic, so the Theil-Sen estimator (Theil, 1950) is probably more reliable than the least-squares fit because it uses medians, which are much less sensitive to outliers. The central Theil-Sen regression line equation for selection 1 is:

$$p = 0.076s - 0.985 \tag{2}$$

The Theil-Sen estimator is associated with the Kendall tau rank correlation (Sen, 1968), which gives a coefficient of 0.64 (0.1 less than the Pearson value). The detailed statistics for the Theil-Sen fit are given in Table 2, for both SEP event selections. The correlation coefficients for the two selections are very similar, differing by only 0.01.

Cycle 23 is of the longest duration (146 months), so a generic cycle is necessarily of duration 13 years (whole or part). When the data for the 6 cycles are combined over this generic cycle

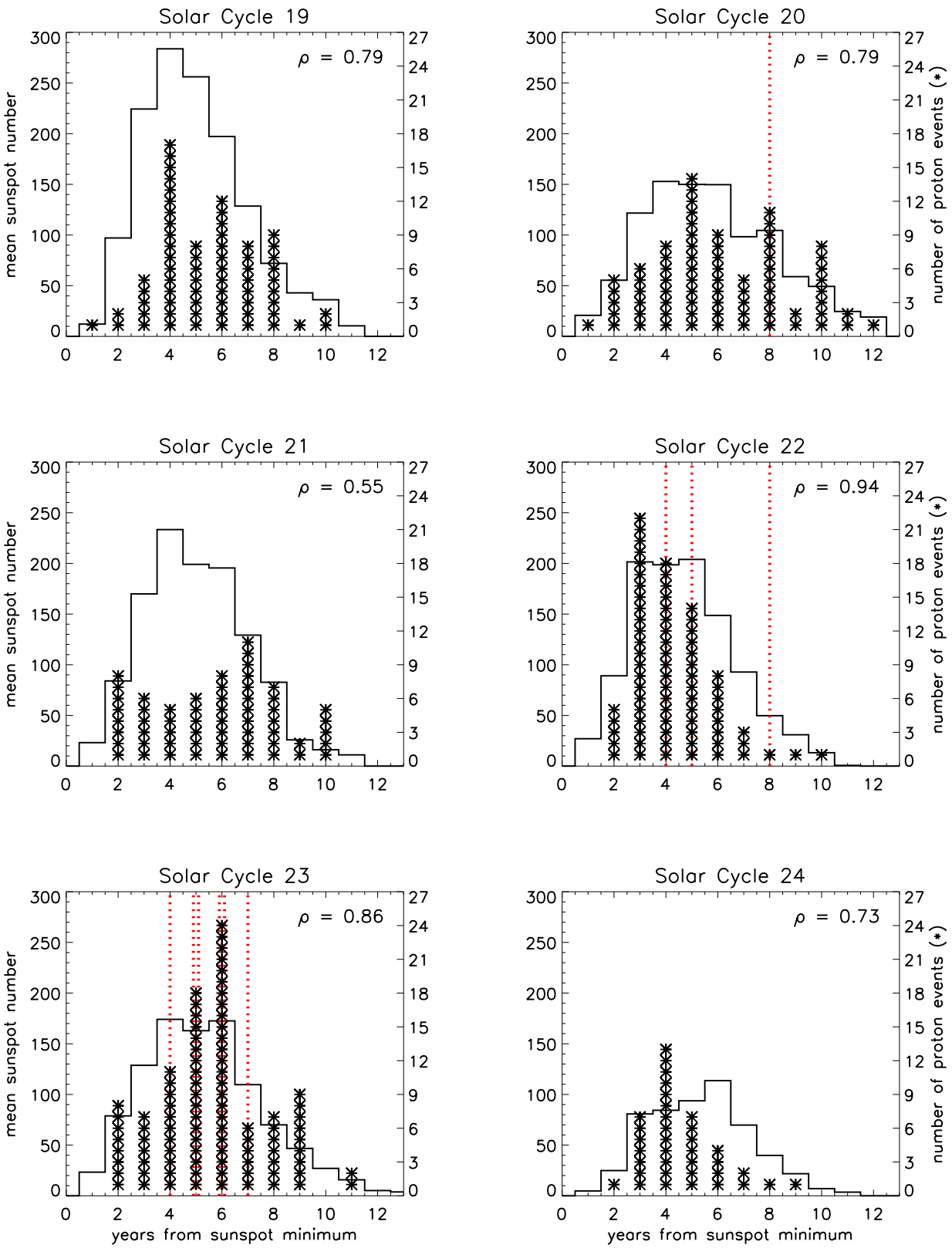

Figure 1: A comparison of mean annual sunspot number and annual number of proton events (selection 1) for solar cycles 19 to 24. The red dotted lines indicate the occurrence of SEP events with peak flux >10000 pfu. (ρ = linear Pearson correlation coefficient.)

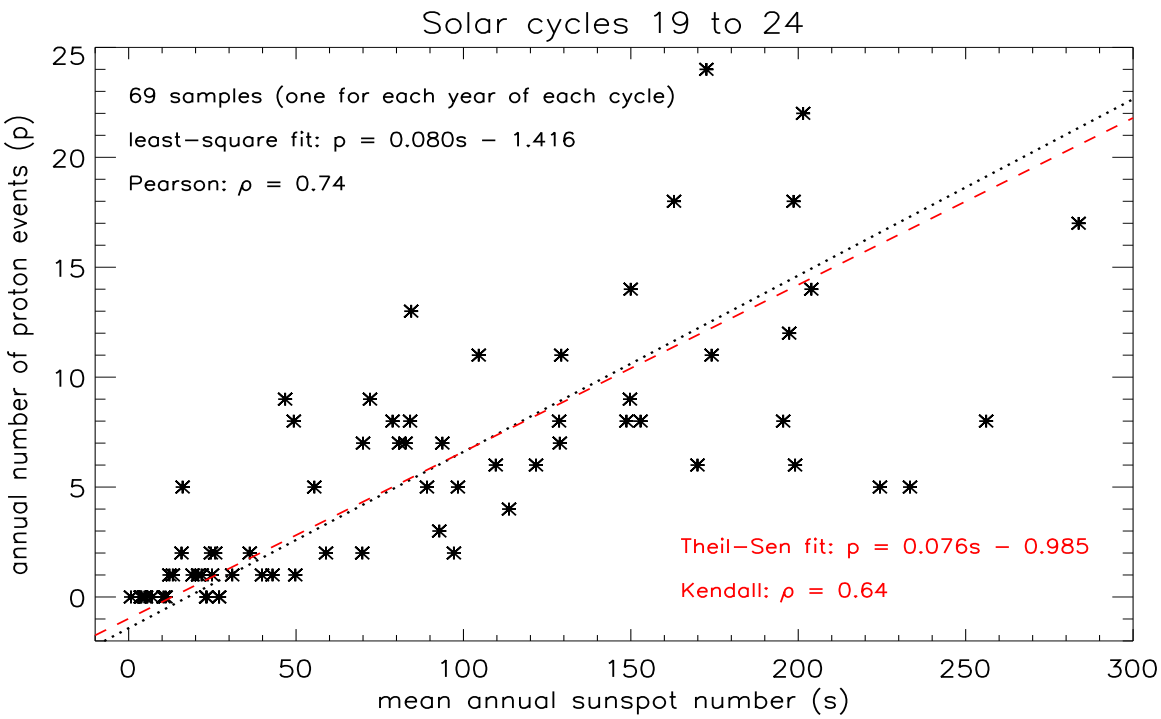

Figure 2: Superposition of results in Figure 1 over solar cycles 19 to 24 (selection 1): least-square fit (dotted); Theil-Sen fit (dashed). (ρ = correlation coefficient. p = annual number of SEPs. s = mean annual sunspot number.)

by summing corresponding years from solar minimum, it appears that there is a very strong relation between the sum of the mean annual sunspot number (S) and the the sum of the annual number of proton events (P) (Figure 3a, showing selection 1). The corresponding scatter plot is shown in Figure 3b, in which the indices adjacent to each data point indicate years after solar minimum, and the correlation ($\rho = 0.97$) is very significant.

The sum of the annual number of SEP events (selection 1) is related to the sum of the mean annual sunspot number (S) according to the central regression line equation for the least-squares fit:

$$P = 0.063S + 0.618 \tag{3}$$

The detailed statistics are given in Table 3, for both SEP event selections. As in Table 2, the

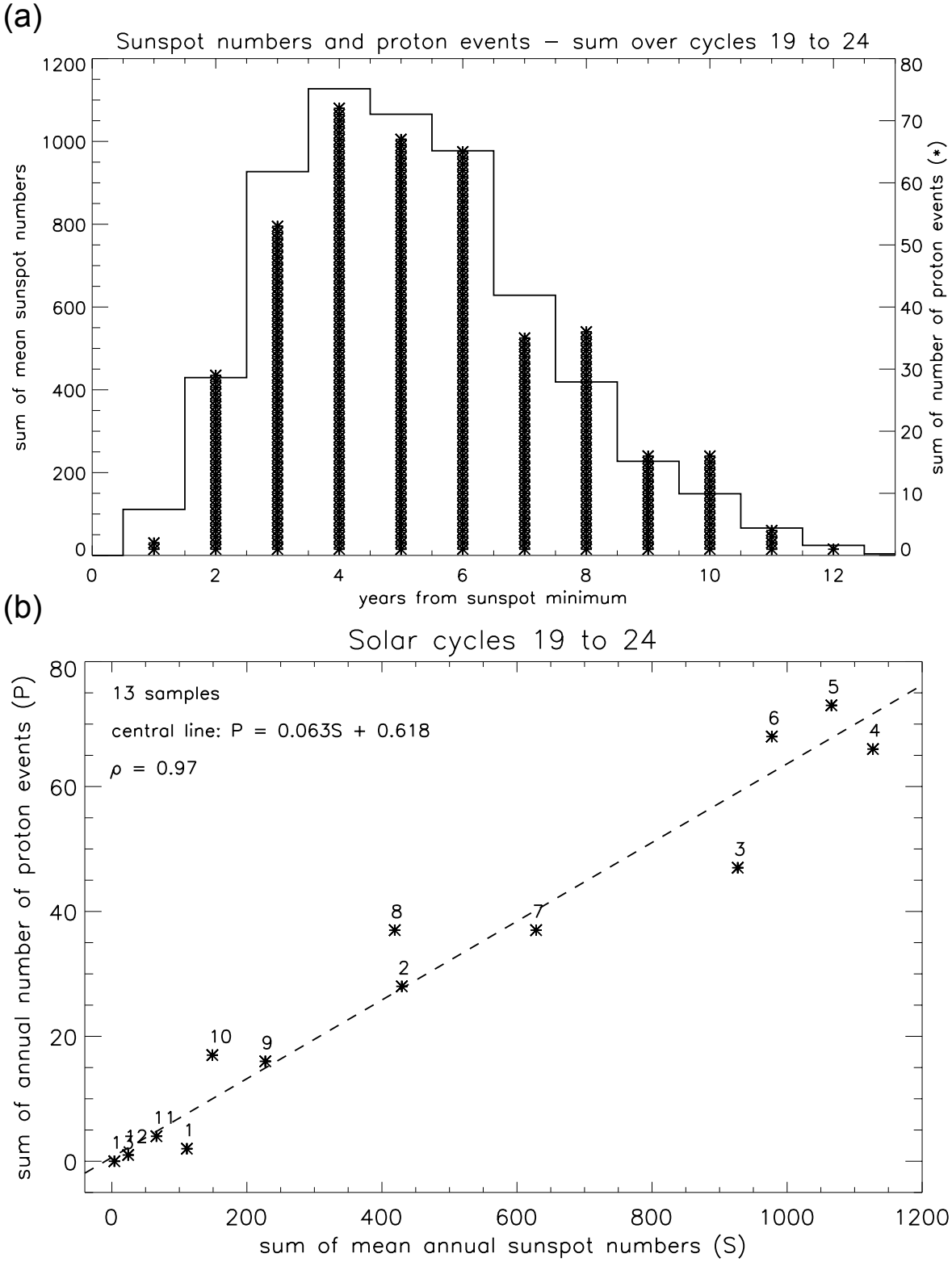

Figure 3: (a) Sum of results in Figure 1 over solar cycles 19 to 24 (selection 1), for corresponding years after solar minimum. (b) Correlation and least-squares fit regression for the results in (a). ρ = linear Pearson correlation coefficient. The indices adjacent to each data point indicate the years after solar minimum.)

Quantity	Selection 1	Selection 2
X on Y	$s = 10.60p + 25.84$	$s = 10.50p + 26.34$
L	3.64	3.43
U	6.60	6.41
Y on X	$p = 0.057s + 0.468$	$p = 0.060s + 0.256$
L	0.000	0.000
U	0.022	0.025
central line	$p = 0.076s - 0.985$	$p = 0.078s - 1.127$
number of samples	69	
ρ	0.64	0.65

Table 2: Theil-Sen regression results for Figure 2, for both SEP event selections. (ρ = Kendall tau rank correlation coefficient. p = annual number of SEPs. s = mean annual sunspot number. L, U = lower and upper 95% confidence intervals for gradient.)

results for the two selections are very similar, the correlation coefficients differing by only 0.01 (selection 2 being 0.98).

4 Solar source of SEP events in cycles 21 to 24.

The SWPC has maintained a catalogue of SEP events since 1975 (to date, covering cycles 21 to 24). The following results are based on this catalogue (selection 1) because the Shea and Smart (1990) list for cycle 21 does not provide solar source locations. In addition, the results for selection 2 (in which the events from November 1997 to September 2005 are replaced by the list provided by Cane et al., 2006) will also be shown (in brackets), where applicable.

Quantity	Selection 1	Selection 2
X on Y	$S = 15.47P - 2.26$	$S = 15.06P - 24.65$
1σ uncertainties	1.07 (m), 42.56 (c)	0.79 (m), 33.44 (c)
Standard error	98.81	75.59
Y on X	$P = 0.061S + 1.382$	$P = 0.064S + 2.555$
1σ uncertainties	0.004 (m), 2.65 (c)	0.003 (m), 2.10 (c)
Standard error	6.23	4.95
central line	$P = 0.063S + 0.618$	$P = 0.065S + 2.096$
number of samples	13	
ρ	0.97	0.98

Table 3: Regression results for Figure 3b. (ρ = linear Pearson correlation coefficient. m = gradient, c = intercept. P = sum of the annual number of SEPs. S = sum of the mean annual sunspot number.)

Of the 259(293) SEP events in selection 1(2), 30(47) have no listed location on the solar disc. The remaining 229(246) events range in longitude from -90° (W limb, to the right when viewed from Earth) to +90° (E limb), and in latitude from 34°N to 43°S (only one sample lying beyond ±40°, at 43°S). (For the purposes of this analysis, the few longitude estimates beyond each limb (e.g. 120°W) are assumed to be 90° E or W, the precise longitude being uncertain. Tests show that this approximation has no effect on the medians, and an insignificant effect on the quartiles.)

Figure 4a shows a histogram, for selection 1, of the longitudes of the 228 ≥10 pfu SEP events within ±40° latitude; the detailed statistics for all latitude ranges and flux thresholds, for both selections, are given in Table 4. Events in the western hemisphere are clearly dominant (median

29(33)°W, with quartiles 16(16)°E and 65(65)°W), which is to be expected because the IMF forms an Archimedian spiral (Parker, 1958) rooted at the photosphere, and the Sun rotates from E to W (see Discussion).

Restricting the population in Figure 4a to higher-flux events (panels b, c and d, with peak flux thresholds ≥100, ≥1000, ≥10000 pfu, respectively) results in a gradual shift in the median longitude of the source towards 0° (named the *helio-meridian* for our purposes). For ≥100 pfu (panel b) the median shifts E by 6(10)° to 23(23)°W, and for ≥1000 pfu (panel c) the median shifts E by a further 16(12)° to 7(11)°W. However, as the threshold increases, there is little change in the quartiles overall. For ≥10000 pfu (panel d) the median shifts E by further 5(9)° to 2(2)°W (quartiles for sample size 9 should be treated with caution).

The effect on the median longitudes of decreasing the latitude range from ±40° to ±[30,20,10]° is illustrated in Figure 5, and it is clear that both data selections give similar results. (Sample sizes <9 are insufficient to provide representative results.)

The median longitudes are all in the western hemisphere (in compliance with the direction of the Parker spiral, see Discussion). Reducing the latitude range from ±40° to ±10° has negligible effect on the longitudes, irrespective of the peak flux threshold, suggesting that variations in the source latitude do not significantly affect the ability of the proton flux to interact with geospace along the Parker spiral (Le at al., 2021). However, as the peak flux threshold increases from ≥10 to ≥10000 pfu, the mean of the median longitudes moves progressively eastward from W32(33)° to W19(20)°, W6(10)° and W2(2)° (demonstrating a progressive shift towards the helio-meridian with increasing flux).

There is no significant difference in the overall distribution of the medians and quartiles between data selections 1 and 2 (panels a and b in Figure 5, and Table 4). Tests also show that the use of three flux *ranges* (for a given peak flux P pfu: $10 \geq P < 100$; $100 \geq P < 1000$; 1000

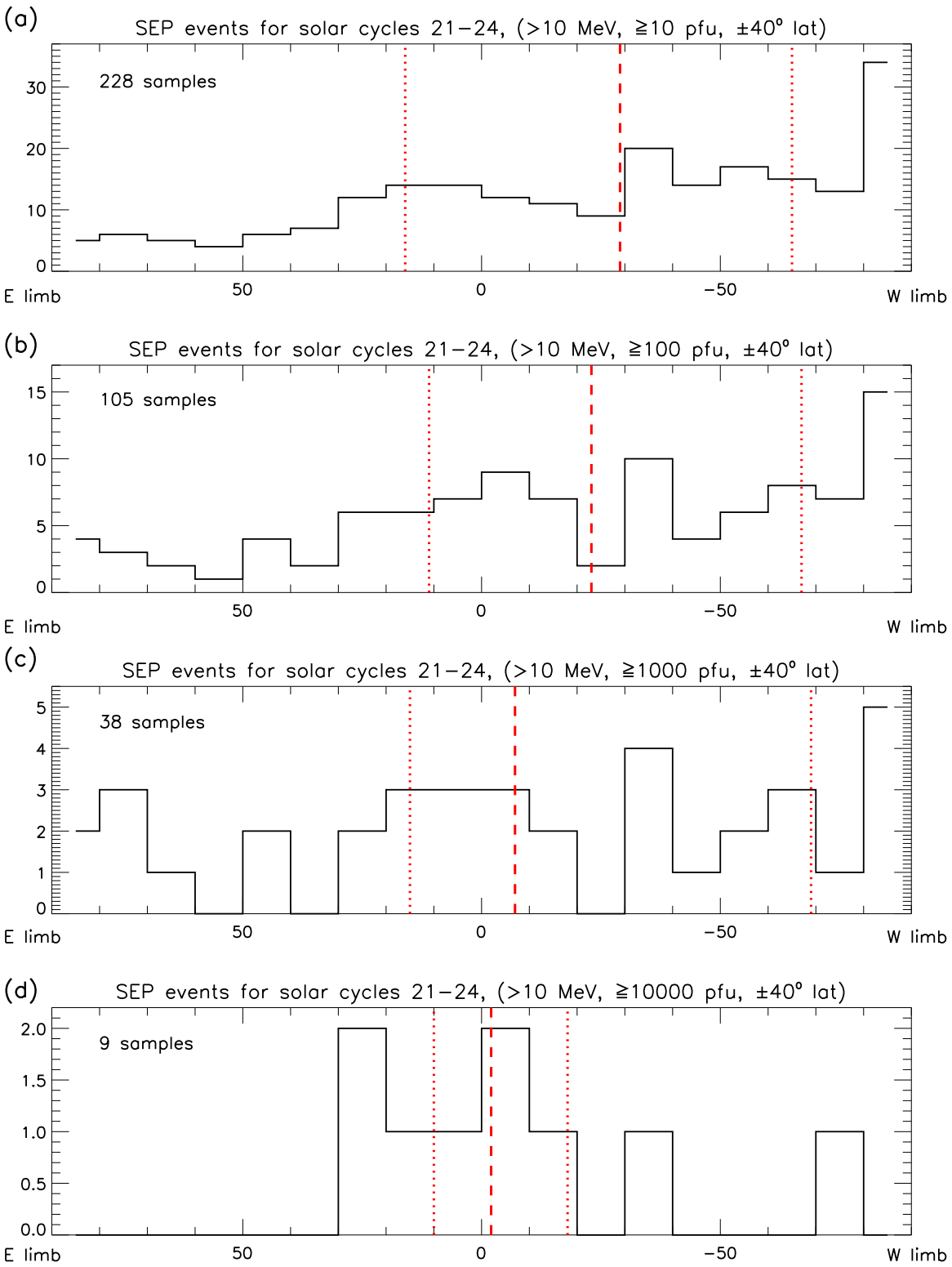

Figure 4: Longitude source of SEP events, within ±40° latitude, for solar cycles 21 to 24 (selection 1): (a) ≥10 pfu; (b) ≥100 pfu; (c) ≥1000 pfu; (d) ≥10000 pfu. (pfu = particle flux units.) In each population, the dashed lines mark the medians, and the dotted lines mark the quartiles.

Population	No. of samples	Easterly quartile	Median	Westerly quartile
$-40° \leq$ latitude $\leq +40°$				
≥10 pfu	228(245)	16(16)E	29(33)W	65(65)W
≥100 pfu	105(114)	11(11)E	23(23)W	67(65)W
≥1000 pfu	38(40)	15(15)E	7(11)W	69(61)W
≥10000 pfu	9(9)	10(10)E	2(2)W	18(18)W
$-30° \leq$ latitude $\leq +30°$				
≥10 pfu	213(220)	16(16)E	29(29)W	64(62)W
≥100 pfu	96(105)	12(11)E	17(17)W	65(64)W
≥1000 pfu	34(36)	15(15)E	5(7)W	70(61)W
≥10000 pfu	9(9)	10(10)E)	2(2)W	18(18)W
$-20° \leq$ latitude $\leq +20°$				
≥10 pfu	167(172)	16(15)E	31(31)W	65(62)W
≥100 pfu	70(77)	15(12)E	17(23)W	65(63)W
≥1000 pfu	21(23)	15(15)E	5(11)W	70(70)W
≥10000 pfu	6(6)	insufficient samples		
$-10° \leq$ latitude $\leq +10°$				
≥10 pfu	64(64)	12(12)E	37(37)W	76(67)W
≥100 pfu	26(30)	24(24)E	17(17)W	67(67)W
≥1000 pfu	7(7)	insufficient samples		
≥10000 pfu	3(3)	insufficient samples		

Table 4: Statistics for the longitude (degrees) of SEP events for solar cycles 21 to 24, for both selections (with selection 2 shown in brackets). Medians and quartiles for sample sizes < 9 are not included. (pfu = particle flux units ($cm^{-2}.s^{-1}.sr^{-1}$). W(est) is the right-hand hemisphere when viewed from Earth.)

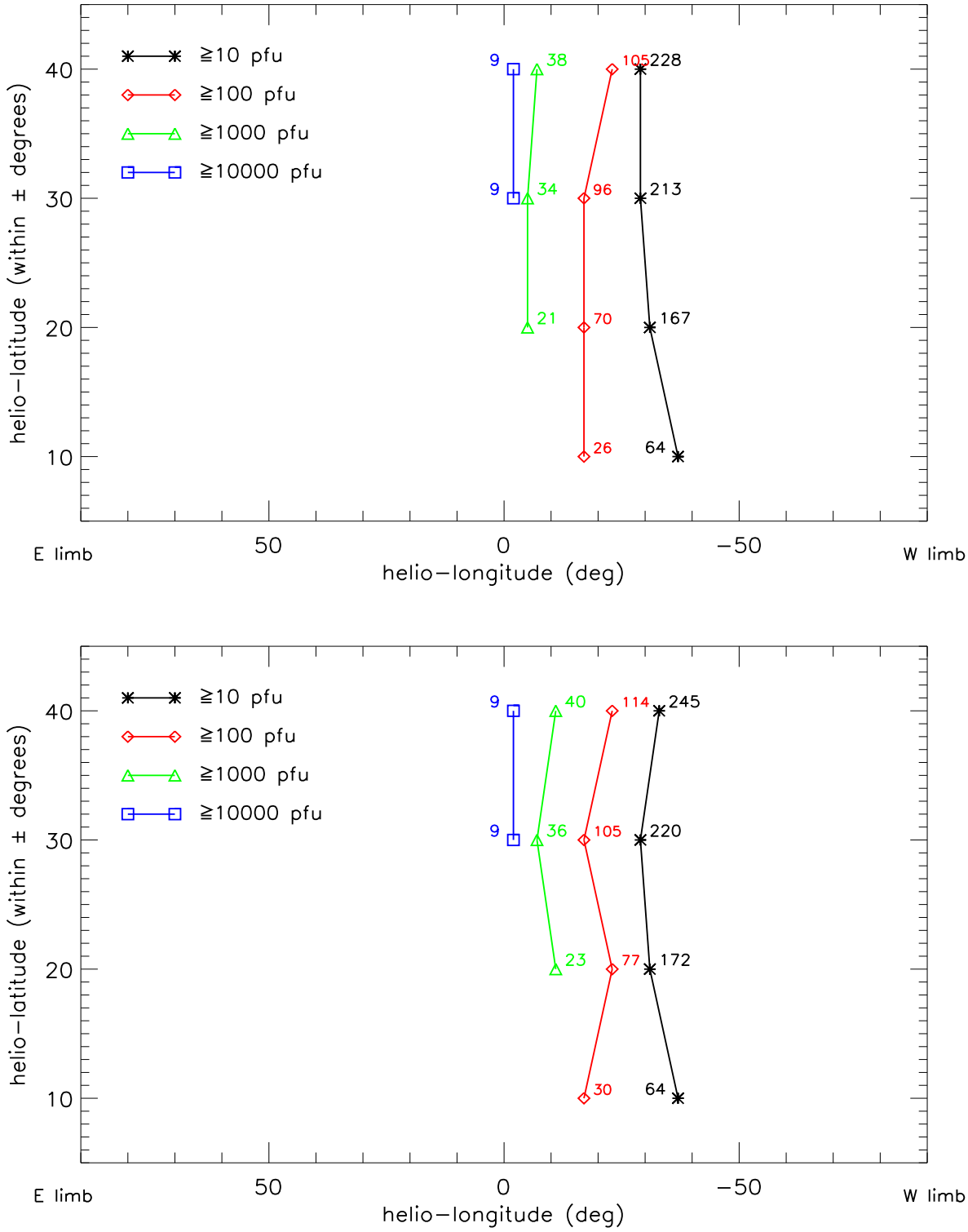

Figure 5: Effect of reducing the latitude range on the median longitudes of the SEP event source locations for the four peak flux thresholds: (a) selection 1; (b) selection 2. The sample sizes are shown alongside each data-point, and the median values are given in Table 4. Data points with number of samples < 9 have been omitted. (pfu = particle flux units)

$\geq$ P $<$ 10000) gave results that were generally similar to those for *thresholds* (P $\geq$ 10000 being the same for both).

5 Discussion

Active regions in the vicinity of sunspot groups are the origin of the vast majority of solar flares and CMEs, which are in turn the source of SEP events. It is therefore not surprising that the annual correlation between SSNs and the occurrence of SEP events is significant in most cases. For strong SEP events (those with flux $\geq$1000 pfu) observed in the period 1976-2018, Le at al. (2021) report that 78% occurred from 2 years before to 3 years after solar maximum. Furthermore, we have demonstrated that when the data from solar cycles 19 to 24 are combined into a single generic cycle the strength of the correlation is remarkable, emphasising the long-term relation between the number of SEP events likely to be incident at the magnetopause and the average annual SSN. Shea and Smart (1995), in a similar comparison for cycles 19 to 21, found a less convincing relation than in this study (which includes, in addition, cycles 22 to 24).

The particles which constitute the solar wind emanate radially from the Sun as it rotates, but the frozen-in magnetic field is rooted at the photosphere. Therefore, any given IMF line represents the locus of all the particles originating at a single point on the solar surface, forming an Archimedean spiral (Parker, 1958). In polar co-ordinates (r, θ), the curve can be described by the equation $r = a + b\theta$, where a represents the solar rotation rate and b the bulk speed (effectively, the speed in the Sun-Earth direction). For example, $b = 250$ (km/s) gives a typical field line with the angle between the spiral and the Sun-Earth radial at 1 AU being $\approx$45°, which is indeed the angle confirmed by observations at L1 during periods when the slow solar wind is dominant.

Because the Sun rotates from E to W (left to right when viewed from the Earth), the resultant

direction of curvature of the IMF means that events originating in the western hemisphere of the Sun are more likely to be detected within geospace than those from the east. Indeed, our results support this principle of E-W asymmetry: out of a total of 41(43) strong SEP events ($\geq$1000 pfu), 25(27) (61%(63%)) originated in the W hemisphere and 16(16) (40%) in the E, in agreement with Le at al. (2021). Using SOHO energetic proton observations from 1996 to 2016 in the energy range 17-22 MeV, Miteva (2019) identified 499 SEP events of known solar origin, of which 74% originated in the W and 26% in the E, demonstrating more pronounced asymmetry.

Not so obvious, however, is the variation in the peak flux relative to the longitude (that is, the higher the flux, the closer is the source location to the helio-meridian, a clear result of this study, and supported by others). Based on the $\geq$1000 pfu SEP events in the SWPC catalogue, Le at al. (2021) report that the source longitude moves towards the helio-meridian as the flux threshold increases. Chen et al. (2014), also using the SWPC catalogue, conclude that all the SEP events with peak flux $\geq$10000 pfu originated from source regions between 30°E and 75°W, and those with $\geq$20000 pfu between 30°E and 20°W, in close agreement with our results. Shea and Smart (1996) also report that solar proton events with high fluences are primarily associated with solar activity near the helio-meridian, and that interplanetary shocks re-accelerate the already enhanced solar proton flux to higher energies than were originally present. These conclusions are based on a sample of 7 >10 MeV high-fluence proton events from 1955 to 1993 and are in general agreement with our result from 233 measurements of peak flux made by the GOES series of satellites during cycles 21 to 24.

Cane et al. (1988) identified 235 proton events with intensity above 3 x 10^{-3} particles $cm^{-2}.s^{-1}.sr^{-1}.MeV^{-1}$ in the energy range 9-23 MeV for the period from mid-May 1967 to the end of 1985, from observations by the IMPs 4, 5, 7, 8 and ISEE 3 spacecraft, all with well-

defined sources. For these events, it was found that with increasing western longitude there was greater likelihood of detecting an event. However, for the subset of 117 shock-associated events, the distribution clearly moved to the east, with a median close to the helio-meridian. Shocks were found to be strongest when observed along the radial from the source region, leading to the conclusion that the highest fluxes are generally observed from sources closer to the helio-meridian. These conclusions by Cane et al. (1988) are also in close agreement with our results.

5.1 Implications for space weather and solar-terrestrial relations

In this field, the prediction of particle events (particularly those with the highest flux) is the ultimate aim, in relation to both (1) long-term strategy with respect to the solar activity cycle, and (2) short-notice warnings to give time for evasive action, following the detection of an event (either from the electromagnetic signature from the solar source, or from the particles themselves). Case 1 applies mainly to the planning of manned deep-space missions, avoiding periods when there is a maximum probability of high-flux events which could be catastrophic to the health of the crew. Case 2 is important for (a) manned space missions (either in deep-space or in low-Earth orbit, when the crew require time to take evasive action, such as by entering a protective enclosure), (b) the prevention of damage to satellites (by re-tasking) and ground-based systems (large-scale conductors, such as power grids and pipelines, affected by the resultant magnetic storms), and (c) the health of air crew on high-altitude, high-latitude flights (to give sufficient time for re-scheduling and re-routing). In this paper, section 3 is more applicable to case (1), and Section 4 to case (2).

By combining all 6 solar cycles, in Section 3 (case 1) it has been demonstrated that SEP events are more likely to occur around solar maximum than solar minimum. This has been reported in previous studies (e.g. Shea and Smart, 1990), but not for cycles 19 to 24 combined,

and this result is striking (Figure 3 and Table 3). Of the 10 high-flux events ($\geq$10000 pfu), there were none in cycles 19, 21 and 24, and most (6) occurred in cycle 23 (red dotted lines in Figure 1, Table 5). Furthermore, 2 occurred in year 4 after solar minimum, 3 in year 5, 2 in year 6, 1 in year 7, and 2 in year 8 (Cheng et al., 2014). It is evident that the optimum time to schedule a deep-space mission is during solar minimum, when it is less likely that the crew will experience a high-flux SEP event. The 9 Apollo lunar missions (8, 10, 11-17) all took place from December 1968 to December 1972, between years 5 and 9 of cycle 20, through solar maximum. At the time, less was known about the source, timing and transmission of these high-energy particle fluxes. In fact, the SEP event on August 4 1972 (with a peak flux of >70000 pfu, by far the highest flux recorded in cycles 19 to 24) occurred between Apollo missions 16 (in April) and 17 (in December). If this event had been coincident with either of these missions the consequences could well have been fatal, particularly when the crews were on the lunar surface. The above factors will presumably have implications for the planning of future deep-space missions, such as to the Moon and Mars.

In Section 4 (case 2), we are concerned with the location of the source of SEP events, not their timing in relation to solar cycle activity. Of particular concern to space weather are high-flux (and by statistical implication, high-energy) events (Le at al., 2014), which we have demonstrated are most likely to be associated with CMEs originating close to the helio-meridian, and which are usually related to shocks (Cane et al., 1988). A high-flux particle event detected at L1 gives no more than about 40 minutes warning before it reaches the magnetopause, insufficient time for evasive action to be taken by astronauts or for technology to be re-tasked. (With the advent of new observing platforms nearer to the Sun, such as the Energetic Particle Detector aboard the Solar Orbiter (Rodrguez-Pacheco et al., 2020), this warning time will be considerably extended. However, such an orbit precludes continuous observations of SEP events headed toward Earth

Cycle	Year in cycle	Date of peak flux	Peak flux (pfu)	Flare (X-ray)	Location	Citation
19	None					
20	8	Aug 4 1972	>70000	X20	≈N10E20	Knipp et al. (2018) Ohshio et al. (1974)
21	None					
22	4	Oct 20 1989	40000	X13	S27E10	Lario and Decker (2002)
	5	Mar 24 1991	43000	X9	S26E28	Smart and Shea (1993)
	8	Feb 21 1994	10000	M4	N09W02	Kahler et al. (1998)
23	4	Jul 15 2000	24000	X5	N22W07	Cane et al (2006)
	5	Nov 09 2000	14800	M7	N05W77	
	5	Sep 25 2001	12900	X2	S16E23	
	6	Nov 06 2001	31700	X1	N06W18	
	6	Nov 24 2001	18900	M9	S15W34	
	7	Oct 29 2003	29500	X17	S16E08	
24	None					

Table 5: SEP events with peak flux≥10000 pfu. (All 10 events involved halo CMEs accompanied by shocks)

unless Solar Orbiter happens to be near the Sun-Earth line.)

However, the electromagnetic signature of the source of a proton event is observed almost instantaneously (in about 8.3 minutes). All of the 10 events in cycles 19 to 24 with peak flux ≥10000 pfu were associated with halo CMEs accompanied by shocks, 3 with M-class flares and 7 with X-class (Table 5, with citations given). The three most intense events (≥40000 pfu) were all related to X-class flares which occurred in the longitude range 10-28°E. All but one of the flares occurred between 28°E and 34°W (the exception being the event on November 9 2000,

an M7 flare at 77°W). From this evidence (necessarily based on a small number of samples), if a flare associated with an active region event is M4 or above, and the source longitude lies between 28°E and 34°W, the particle flux is likely to be the result of a CME shock-front, the effects of which could have very serious consequences within geospace (Cohen, 2006). However, depending on the velocity of the ejecta, the proton flux takes about 1 to 2 days to reach the magnetopause, which gives sufficient time for evasive action to be taken.

6 Summary

The quantitative results in this summary apply to SEP event selection 1, but in qualitative terms there is negligible distinction between selections 1 and 2.

1. When solar cycles 19 to 24 are superposed (69 samples, 1 per year of each solar cycle), the mean annual sunspot number (s) and the annual number of SEP events (p) are reasonably well correlated (Kendall tau rank correlation, $\rho = 0.64$) with Theil-Sen estimator $p = 0.076s - 0.985$.

2. When cycles 19 to 24 are combined to give a generic solar cycle (13 samples, 1 per year), the sum of the mean annual sunspot number (S) and the sum of the annual number of SEP events (P) are very strongly correlated (Pearson linear correlation, $\rho = 0.99$) with least-squares fit $P = 0.063S + 0.618$.

3. For SEP event sources with a given peak flux threshold, the helio-longitude is almost constant within±40° helio-latitude.

4. However, with increasing flux threshold the median helio-longitude of the source migrates eastward towards 0° (specifically, from 32°W for ≥10 pfu, 19°W for ≥100 pfu, 6°W for ≥1000 pfu, and 2°W for ≥10000 pfu).

5. Of the 10 events in cycles 19 to 24 with peak flux ≥10000 pfu, all occurred between years 4 and 8 after solar minimum, all were the result of M- or X-class flares with associated halo CMEs and shock fronts, and the three most intense events (≥40000 pfu) were all related to X-class flares which occurred in the longitude range 10-28°E.

6. These results support and extend previous work by the cited authors, and have implications for the long-term planning of manned deep-space missions, solar-terrestrial relations and the effects of space weather within geospace.

Acknowledgements

The authors wish to thank the providers of the following web-based data services for the provision of the SSN, and SEP data:

- World Data Centre for Sunspot Index and Long-term Solar Observations, Royal Observatory of Belgium, Brussels:
  sidc.oma.be/silso/home/

- Space Weather Prediction Center, NOAA, Boulder, USA:
  ftp.swpc.noaa.gov/pub/indices/SPE.txt

Appendix For clarification, Table 6 summarises the SEP event selection criteria, the sample numbers, and their location throughout the paper.

	SEP event group	No. of samples		Section, Table, Figure
1	Cycles 19 and 20 (Shea & Smart, 1990)	137		S2.2, T1
2	Cycles 19 to 24	396 (430)		S3, T1
3	Cycles 21 to 24	259 (293)	$2-1$	S4.1, T1
4	Cycles 21 to 24 (no known source location and/or flux)	30 (47)		S4.1
5	Cycles 21 to 24 (known source location and flux)	229 (246)	$3-4$	S4.1
6	Cycles 21 to 24 ($-40° >$ latitude $> +40°$)	1(1)		S4.1
7	Cycles 21 to 24 ($-40° \leq$ latitude $\leq +40°$)	228 (245)	$5-6$	S4.1, T4, F4, F5

Table 6: Selection criteria for the SEP events (S = section. T = table. F = figure).

References

Cane, H.V., Reames, D.V., von Rosenvinge, T.T., The role of interplanetary shocks in the longitude distribution of solar energetic particles. Journal of Geophysical Research, Volume 93, Issue A9, p. 9555-9567, 10.1029/JA093iA09p09555, September 1988.

Cane, H.V., Mewaldt R.A., Cohen C.M.S., von Rosenvinge, T.T., Role of flares and shocks in determining solar energetic particle abundances, Journal of Geophysical Research, Volume 111, A06S90, 10.1029/2005JA011071, 2006.

Cheng L-b., Le G-m., Lu Y-p., Chen M-h., Li P., Yin Z-q., Analysis of the Properties of Super Solar Proton Events and Associated Phenomena, Chinese Astronomy and Astrophysics, 38, 439447, 2014.

Clette, F., Svalgaard, L., Vaquero, J.M., Cliver, E. W., Revisiting the Sunspot Number. A 400-Year Perspective on the Solar Cycle, Space Science Reviews, Volume 186, Issue 1-4, pp. 35-103. DOI: 10.1007/s11214-014-0074-2, 2014

Clette, F., Lefèvre, L., The New Sunspot Number: assembling all corrections, Solar Physics, 291, DOI: 10.1007/s11207-016-1014-y, 2016a

Clette, F., Lefèvre, L., Cagnotti, M., Cortesi, S., Bulling, A., The Revised Brussels-Locarno Sunspot Number (1981 - 2015), Solar Physics, 291, DOI: 10.1007/s11207-016-0875-4, 2016b

Clette, F., Cliver, E.W., Lefèvre, L, Svalgaard, L., Vaquero, J.M., Leibacher, J.W., Preface to Topical Issue: Recalibration of the Sunspot Number, Solar Phys., 291, DOI: 10.1007/s11207-016-1017-8, 2016c

Cliver E.W., Clette F., Svalgaard L., Recalibrating the Sunspot Number (SSN): The SSN Workshops, Cent. Eur. Astrophys. Bull., 37, 401416, 2013.

Cohen, C.M.S. Observations of energetic storm particles: An overview. Solar Eruptions and Energetic Particles, ed. Gopalswamy N., Mewaldt R., and Torsti J., Geophysical Monograph 165, 275-282, DOI:10.1029/165GM26, 2006.

Forbush S.E., Three Unusual Cosmic-Ray Increases Possibly Due to Charged Particles from the Sun, Physical Review, vol.70, iss.9-10, p. 771-2, DOI: 10.1103/PhysRev.70.771, November 1946.

Gabriel, S., Evans, R., Feynman, J., Periodicities in the Occurrence of Solar Proton Events, Solar Physics, vol.128, pp.415-422, 1990.

Ivanov V.G., Shape of the 11-Year Cycle of Solar Activity and the Evolution of Latitude Characteristics of the Sunspot Distribution, Geomagnetism and Aeronomy, Volume 58, Issue 7, pp.930-936, December 2018.

Kahler, S.W., Cane H.V., Hudson H.S., Kurt V.G., Gotselyuk Y.V., MacDowell R.J., Bothmer, V., The solar energetic particle event of April 14,1994, as a probe of shock formation and

particle acceleration, Journal of Geophysical Research, vol.103, no.A6, pp.12069-12076, June 1 1998.

Knipp D.J., Fraser B.J., Shea M.A., Smart D.F., On the Little-Known Consequences of the 4 August 1972 Ultra-Fast Coronal Mass Ejecta: Facts, Commentary, and Call to Action, Space Weather, 16, 16351643, https://doi.org/ 10.1029/2018SW002024, 2018.

Lario D., Decker R.B., The energetic storm particle event of October 20, 1989, Journal of Geophysical Research, vol.29, no.10, 1393, 10.1029/2001GL014017, 2002.

Le G-M., Yang X, Ding L., Liu Y, Lu Y., Chen M., Solar cycle distribution of strong solar proton events and the related solar-terrestrial phenomena, Astrophys. Sp. Sci., 352:403408 DOI 10.1007/s10509-014-1964-1, 2014.

Le G-M., Zhao M-X, Qi-Li, Liu G-A, MaoT., Xu P-G, Characteristics of source locations and solar cycle distribution of the strong solar proton events (1000 pfu) from 1976 to 2018, MNRAS 502, 20432048, 2021.

Miteva R., On the solar origin of in situ observed energetic protons, Bulgarian Astronomical Journal 31, 2019.

Ohshio, M., Solar-terrestrial disturbances of August 1972. Solar x-ray flares and their corresponding sudden ionospheric disturbances. Journal of the Radio Research Laboratories (in Japanese). Koganei, Tokyo. 21 (106): 311340, 1974.

Parker, E.N., Dynamics of the Interplanetary Gas and Magnetic Fields, Astrophysical Journal, vol.128, p.664, 1958.

Rodrguez-Pacheco, J. ; Wimmer-Schweingruber, R. F. ; Mason, G. M. ; Ho, G. C. ; Sánchez-Prieto, S. ; Prieto, M. ; Martn, C. ; Seifert, H. ; Andrews, G. B. ; Kulkarni, S. R. ; Panitzsch, L.

; Boden, S. ; Böttcher, S. I. ; Cernuda, I. ; Elftmann, R. ; Espinosa Lara, F.; Gómez-Herrero, R.; Terasa, C. ; Almena, J. ; Begley, S. ; Böhm, E. ; Blanco, J. J. ; Boogaerts, W. ; Carrasco, A. ; Castillo, R. ; da Silva Farina, A. ; de Manuel González, V. ; Drews, C. ; Dupont, A. R. ; Eldrum, S. ; Gordillo, C. ; Gutiérrez, O. ; Haggerty, D. K. ; Hayes, J. R. ; Heber, B. ; Hill, M. E. ; Jüngling, M. ; Kerem, S. ; Knierim, V. ; Köhler, J. ; Kolbe, S. ; Kulemzin, A. ; Lario, D. ; Lees, W. J. ; Liang, S. ; Martnez Helln, A. ; Meziat, D. ; Montalvo, A. ; Nelson, K. S. ; Parra, P. ; Paspirgilis, R. ; Ravanbakhsh, A. ; Richards, M. ; Rodrguez-Polo, O. ; Russu, A. ; Sánchez, I. ; Schlemm, C. E. ; Schuster, B. ; Seimetz, L. ; Steinhagen, J. ; Tammen, J. ; Tyagi, K. ; Varela, T. ; Yedla, M. ; Yu, J. ; Agueda, N. ; Aran, A. ; Horbury, T. S. ; Klecker, B. ; Klein, K. -L. ; Kontar, E. ; Krucker, S. ; Maksimovic, M. ; Malandraki, O. ; Owen, C. J. ; Pacheco, D. ; Sanahuja, B. ; Vainio, R. ; Connell, J. J. ; Dalla, S. ; Dröge, W. ; Gevin, O. ; Gopalswamy, N. ; Kartavykh, Y. Y. ; Kudela, K. ; Limousin, O. ; Makela, P. ; Mann, G. ; Önel, H.; Posner, A. ; Ryan, J. M. ; Soucek, J. ; Hofmeister, S. ; Vilmer, N. ; Walsh, A. P. ; Wang, L. ; Wiedenbeck, M. E. ; Wirth, K. ; Zong, Q., The Energetic Particle Detector: Energetic particle instrument suite for the Solar Orbiter mission, Astronomy & Astrophysics, Volume 642, id.A7, 35, DOI: 10.1051/0004-6361/201935287, October 2020.

Sen, P. K., Estimates of the regression coefficient based on Kendall's tau, Journal of the American Statistical Association, 63 (324): 13791389, doi:10.2307/2285891, JSTOR 2285891, MR 0258201, 1968.

Shea, M.A., Smart, D.F., A summary of major solar proton events, Solar Physics. 127, 298, 1990.

Shea, M.A. and Smart, D.F., March 1991 Solar-Terrestrial Phenomena and Related Technological Consequences, 23rd International Cosmic Ray Conference, 19-30 July, 1993 at University

of Calgary, Alberta, Canada, vol.3, p.739, 1993.

Shea, M.A., Smart, D.F., History of solar proton event observations, Nuclear Physics B (Proc. Suppl.) 39A, 16-25, 1995.

Shea, M.A., Smart, D.F., Solar Proton Fluxes as a Function of the Observation Location with respect to the Parent Solar Activity, Adv.Space Res. vol.17, no.4/5, pp.225-228, 1996.

Theil, H., A rank-invariant method of linear and polynomial regression analysis. I, II, III, Nederl. Akad. Wetensch., Proc., 53: 386392, 521525, 13971412, MR 0036489, 1950.

van Speybroeck, L.P., Krieger, A.S., Vaiana, G.S., X-Ray Photographs of the Sun on March 7, 1970, Nature, vol. 227, pp. 818., 1970.